Particle Image Velocimetry Measurements of Wire-nonparallel Plates Type Electrohydrodynamic Gas Pump

Marek Kocik, Janusz Podliński, Jerzy Mizeraczyk
Centre for Plasma and Laser Engineering,
The Szewalski Institute of Fluid Flow Machinery,
Polish Academy of Sciences,
Fiszera 14, 80-952 Gdańsk, Poland

and **Jen-Shih Chang**
McIARS & Department of Engineering Physics,
McMaster University,
Hamilton, Ontario, L8S 4M1, Canada

ABSTRACT

2D Particle Image Velocimetry (PIV) measurements were performed in a wire-nonparallel plates type electrohydrodynamic (EHD) gas pump. Using simultaneously two CCD cameras allowed obtaining high resolution vector maps which illustrate the flow patterns generated inside the EHD gas pump.

Index Terms—Particle Image Velocimetry, electrohydrodynamic pump, Corona discharges, Non-thermal plasmas

1 INTRODUCTION

WHEN a strong electric field is applied between high voltage and grounded electrodes in a gas medium, a corona discharge is formed by ionization of the gas molecules. Thus ion flux along the electric field transfers its momentum to the neutral molecules and results in the so-called ionic wind or an electrohydrodynamically induced gas flow. When the electrodes configuration forms an unsymmetrical electric field distribution, the unidirectional gas flow can be generated, i.e. electrohydrodynamic (EHD) gas pumping occurs. A several electrode geometries have been proposed for EHD gas pumps such as needle-to-mesh, needle-to-ring, wire-to-rod, wire-nonparallel plates, etc. [1-7].

In this work, the performance of a wire-non-parallel plate push fan (PF) type EHD gas pump is studied by Particle Image Velocimetry (PIV) for measurement of the flow patterns. It was already demonstrated that the PIV technique is capable of measuring the flow velocity fields in the conditions typical of the EHD pumps [8-11].

The dimensions of EHD gas pump as well as electrodes configuration are the same as reported in [7], where the flow characteristics (pressure drop and mean flow velocity at the pump exit) of the EHD gas pump were given. These characteristics show that without detailed study of the flow patterns inside EHD gas pumps, only general conclusions such as the generated flow is turbulent or re-circulating laminar could be made. Therefore, to understand the flow behavior in the EHD gas pump it is necessary to investigate in detail the velocity flow patterns near flow driven electrodes.

2 EXPERIMENTAL SET-UP

The EHD gas pump used in this experiment was a box made of transparent acrylic plates of a thickness of 10 mm. The internal dimensions of the box were 120 mm x 35 mm x 50 mm. Two engraved slits with 3° convergent angle were made in two sidewalls (Figure 1). Two acrylic plates covered with grounded electrodes could slide-in and off in the engraved slits. When these plates with plane grounded electrodes were placed in the slits, the cross sections of the EHD pump inlet and outlet were of 35 mm x 24 mm and 35 mm x 12 mm, respectively. The grounded electrodes (75 mm x 35 mm) were made of aluminum tape of a thickness of 50 μm. They could be shifted along the acrylic plate base, changing their positions in respect to the wire discharge electrode. The discharge electrode was a stainless-steel wire of a diameter of 0.23 mm and width of 35 mm, placed parallel to the plane grounded electrodes. The position of the corona wire electrode was always 60 mm from the EHD pump outlet. Two positions of the grounded electrodes were set: 6 mm from the EHD pump inlet (the pump type called PF-A) and 36 mm from the EHD pump inlet (PF-B) (Figure 1). Two acrylic boxes (110 mm x 140 mm x 400 mm) were connected inlet and exit sections of the EHD gas pump then both ends were

Manuscript received on 21 April 2008, in final form 24 July 2008.

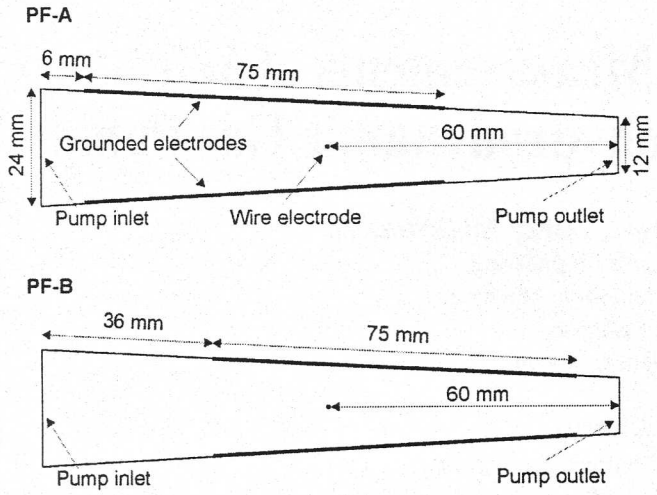

Figure 1. EHD gas pump dimensions and electrode geometry (PF-A and PF-B).

connected by a plastic tube (diameter = 6 cm). to form a closed flow loop.

dc high voltage was supplied to the wire electrode through a ballast resistor (10 MΩ) from a dc power supply (Spellman SL300) (Figure 2). The applied voltage was measured using a high voltage probe (Tektronix, P6015A).

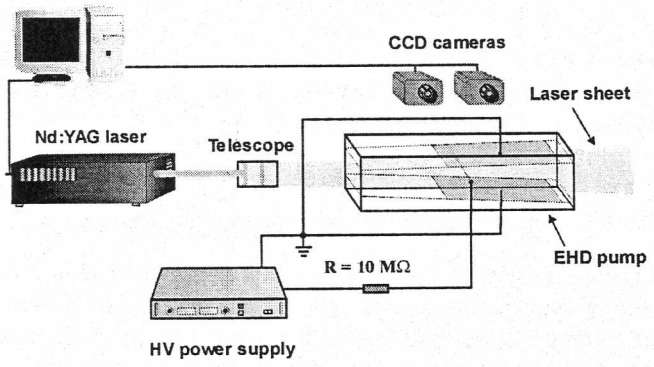

Figure 2. PIV experimental set-up.

The PIV measurements were carried out using a PIV equipment consisted of a twin second harmonic Nd-YAG laser system (λ=532 nm, pulse energy 50 mJ), imaging optics, two CCD cameras and PC computer equipped with Dantec Flow Manager software (Figure 2). The laser sheet, which defines the measuring plane, of a thickness of 1 mm, formed from the Nd-YAG laser beam by a cylindrical telescope, was introduced into the EHD gas pump. Cigarette smoke particles (0.5-1 μm diameter [12]) were used as seed tracers. The influence of the seed particles on the EHD flow is discussed in [14] together with optimization of particle size and density to exert minimal influence on the flow. The PIV images were recorded by two Flow Sense M2 CCD cameras simultaneously. Each camera was capable of capturing two PIV images with minimum time separation of 2 μs. The CCD camera active element size was 1186 x 1600 pixels. The captured images were transmitted to the PC computer for digital analysis. The observation area of each camera was a rectangle of 4.5 cm x 6 cm.

The both observation areas were set as shown in Figure 3, with 1 cm overlapping region. During the PIV measurements, two flow velocity vector maps were created, one for each observation area. Since both cameras recorded images simultaneously and the overlapping region was relatively wide, stitching the vector maps was possible. The stitching was made after averaging over 100 measurements into one flow velocity vector map which covered almost the whole length of the EHD gas pump. Using two cameras allowed obtaining the higher resolution images and resulting vector maps were more detailed.

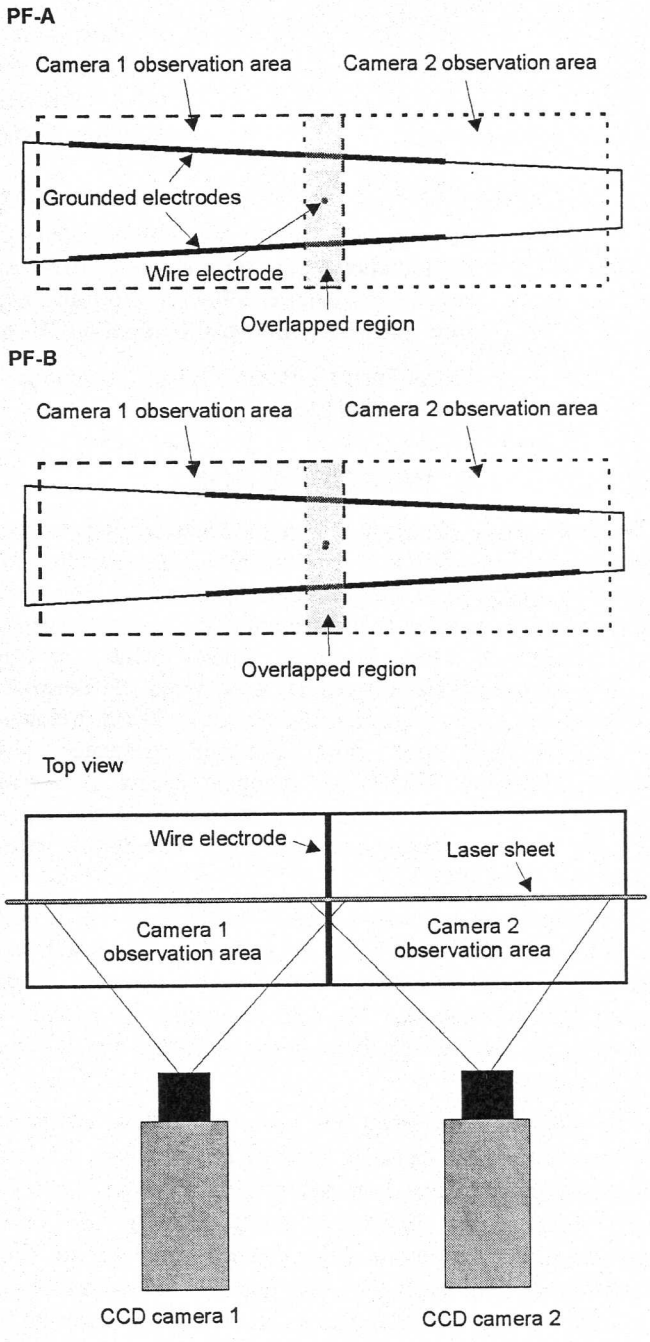

Figure 3. PIV measurement observation areas for PF-A and PF-B pumps.

Based on the measured vector maps, the existent flow streamlines of a hypothetical 2-D flow were calculated.

3 Results

The time averaged corona current-voltage characteristics for PF-A and PF-B type EHD gas pumps for negative and positive applied voltage polarities are shown in Figure 4.

The corona onsets started above 6 kV of the applied voltage. For the voltages of 6-8 kV, the EHD recirculation flow pattern

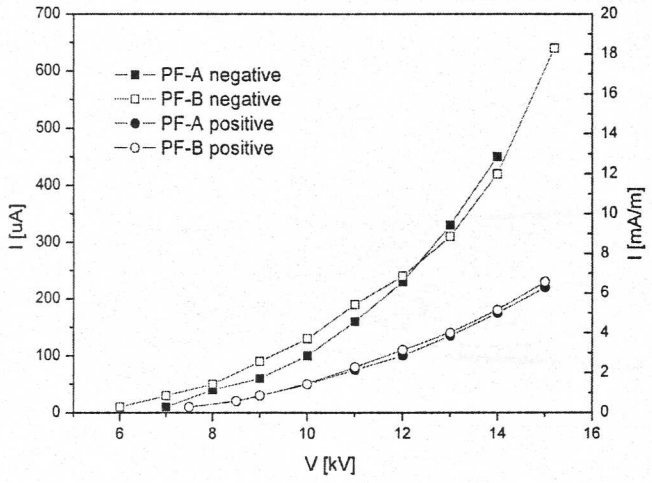

Figure 4. Time averaged corona current–voltage characteristics of PF-A and PF-B type EHD gas pumps for negative and positive applied voltage polarities.

appeared near the corona wire, however no significant unidirectional flow could be observed. The overall unidirectional flow towards pump exit occurred for voltages higher than 8-9 kV.

The flow velocity vector maps and the corresponding flow streamlines in PF-A type EHD gas pump at positive voltage polarity 8 kV and 15 kV are shown in Figure 5. It can be observed that for a voltage of 8 kV (Figures 5a to 5b) a pair of vortices in the upstream region (in respect to the wire electrode position) and another pair of vortices in the downstream region are formed. The generated flow velocity reaches a value of 0.6 m/s near the discharge region. However, the x-component maximum velocity at the inlet and exit sections of EHD gas pump is only 0.1 and 0.18 m/s, respectively. The reason of this weak pumping effect is the formation of vortices which may block the flow along the EHD gas pump as was suggested by Chun and al [13]. The flow velocity vector map and the corresponding streamlines at 15 kV are shown in Figures 5c-5d. It can be seen from these figures that the upstream vortices were pushed to downstream direction, closer to the discharge wire electrode. The downstream vortices were scattered by the EHD flow, which is stronger than that at 8 kV. However, still the significant slow down of the flow existed in the central part of downstream region. The flow velocity up to 1.8 m/s in the discharge region was measured. At the EHD gas pump inlet and exit section, the maximum flow velocities were 0.47 and 0.96 m/s, respectively.

The flow velocity vector maps and the corresponding flow streamlines in PF-A type EHD gas pump for negative voltage polarity (8 kV and 14 kV) is shown in Figure 6. For the negative polarity, increasing the applied voltage above 14 kV often resulted in the spark discharge. Therefore, for this polarity the PIV measurement was performed only up to 14 kV. However, when comparing the positive with the negative polarity discharge one should notice that the time averaged discharge current at the negative polarity is much higher than that at the positive one for the fixed operating voltage.

Table 1. The maximum velocity values measured at inlet and exit of EHD gas pump.

	Applied voltage V [kV]	Max. inlet velocity U_x [m/s]	Max. exit velocity U_x [m/s]	Flow rate Q [L/min]
PF-A Positive	8	0.1	0.18	5
	12	0.32	0.62	16
	15	0.48	0.92	24
PF-A Negative	8	0.14	0.28	7
	12	0.37	0.64	19
	14	0.47	0.96	24
PF-B Positive	8	0.09	0.14	4.5
	12	0.28	0.58	14
	15	0.39	0.76	20
PF-B Negative	8	0.08	0.2	4
	12	0.28	0.54	14
	14	0.33	0.56	17

At 8 kV, the flow patterns formed in PF-A type EHD gas pump for both voltage polarities are very similar (Figures 5a-5b and Figures 6a-6b). However, at the negative polarity downstream vortices are stronger and the upstream vortices are weaker than that of corresponding one at the positive polarity. For higher applied voltages, the difference in vortices size is even more visible (Figures 5c-5d and Figures 6c-6d). At the negative polarity, the maximum flow velocity x-component at the pump inlet and exit sections were 0.48 and 0.92 m/s, respectively. This is very similar to those obtained for the positive voltage polarity.

Figure 7 shows the flow streamlines for PF-B type EHD gas pump for the positive (Figures 7a, 7c; 8 kV and 15 kV) and the negative (Figures 7b, 7d; 8 kV and 14 kV) voltage polarities. Also for this EHD gas pump type, upstream and downstream vortices are formed, and similarly to PF-A type pump, the upstream vortices are stronger for the positive voltage polarity and the downstream vortices are stronger for the negative voltage polarity. It can be noticed that both, upstream and downstream vortices are more pronounced for PF-B than for PF-A type EHD gas pump (Figures 5-7). For both types of the EHD gas pump, PF-A and PF-B, the number and strength of the vortices decrease with increasing operating voltage, regardless the voltage polarity. However, even for the highest applied voltage [i.e., 15 kV for the positive polarity (Figure 7c) and 14 kV for the negative polarity (Figure 7d)] the vortices are relatively strong in the downstream region of PF-B type pump. This may cause a lower maximum velocities obtained at the inlet and exit sections of PF-B type EHD gas pump (Table 1).

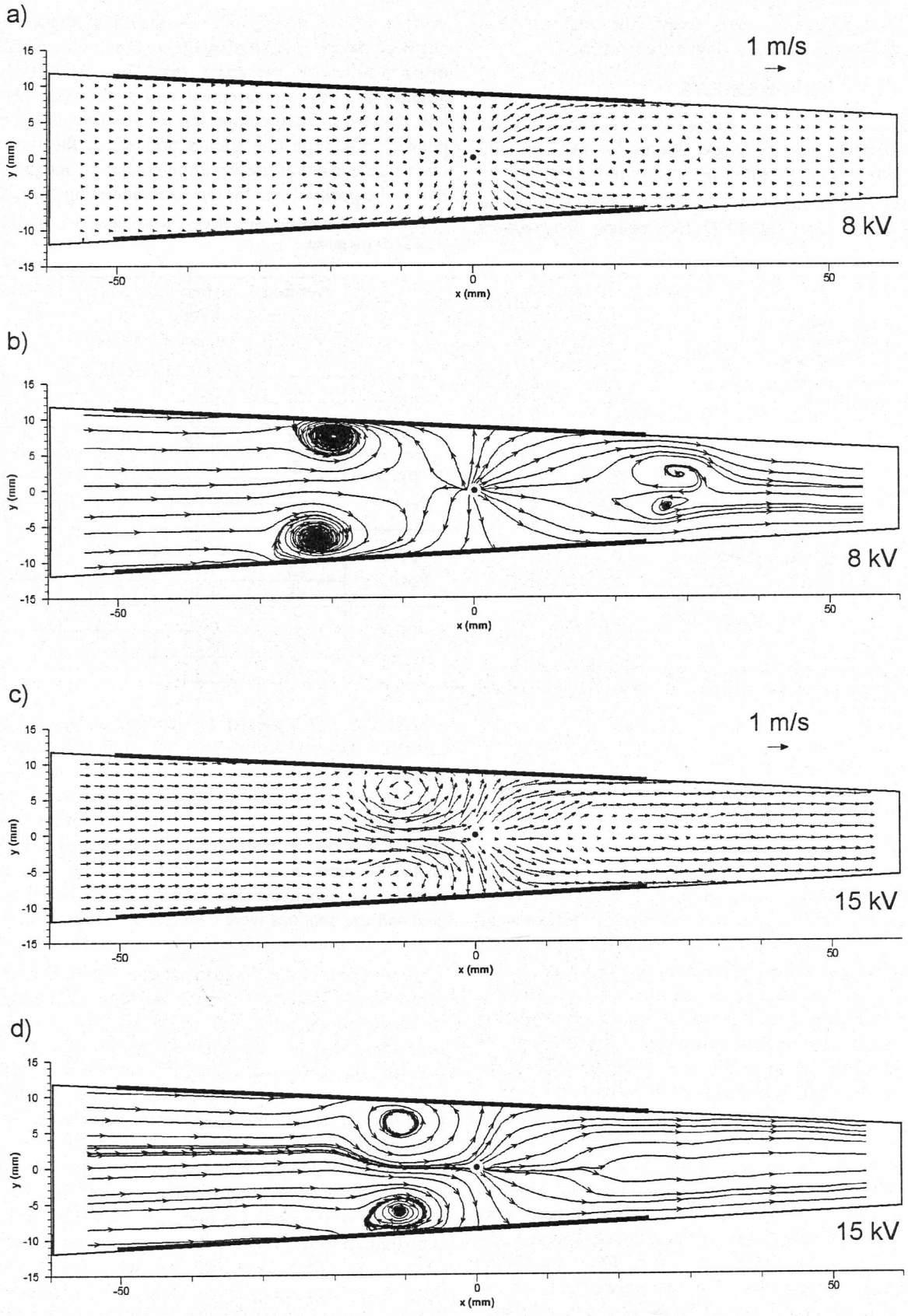

Figure 5. Flow velocity vector maps (a, c) and the corresponding flow streamlines (b, d) for PF-A type EHD gas pump for positive applied voltages.

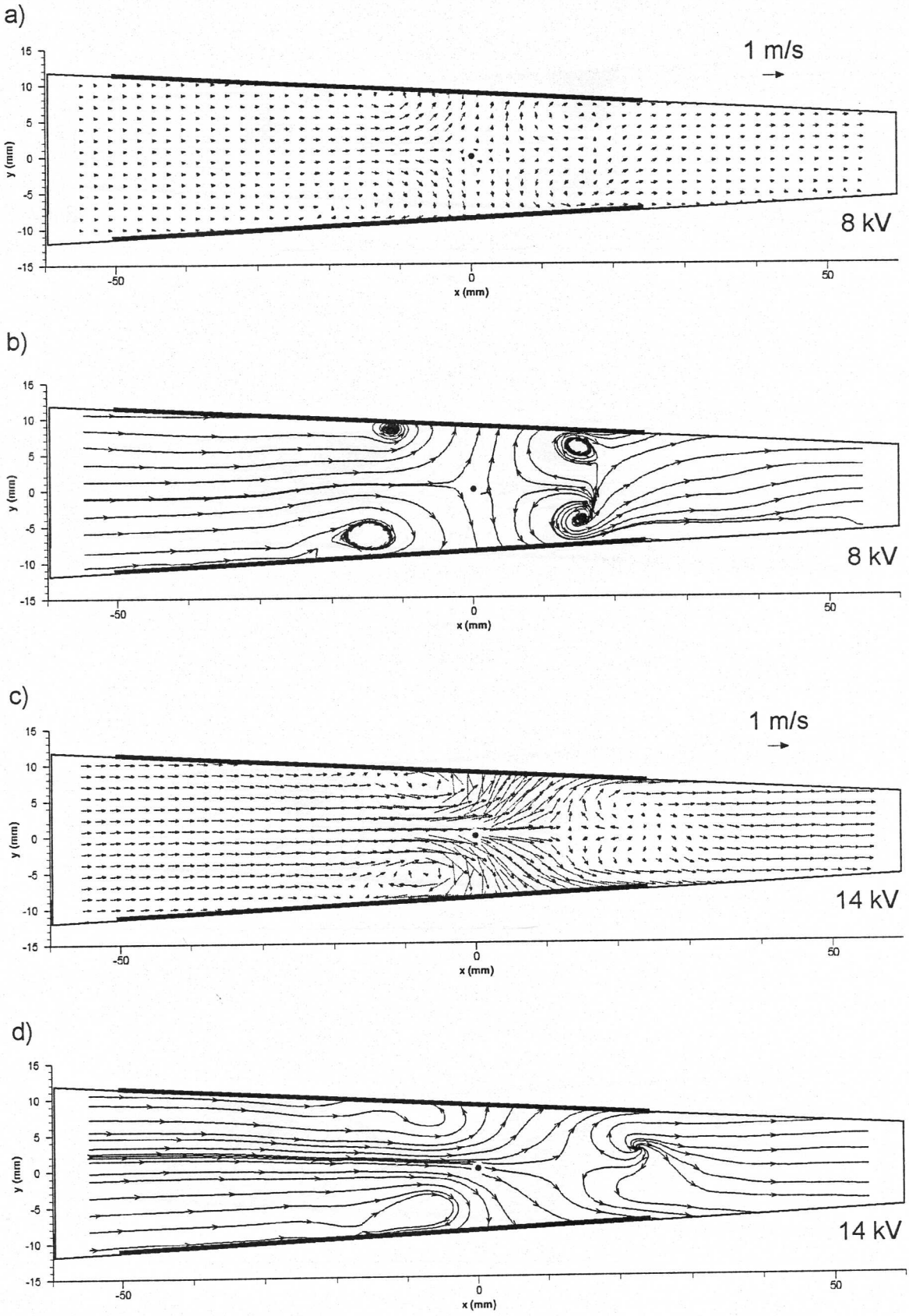

Figure 6. Flow velocity vector maps (a, c) and the corresponding flow streamlines (b, d) for PF-A type EHD gas pump for negative applied voltages.

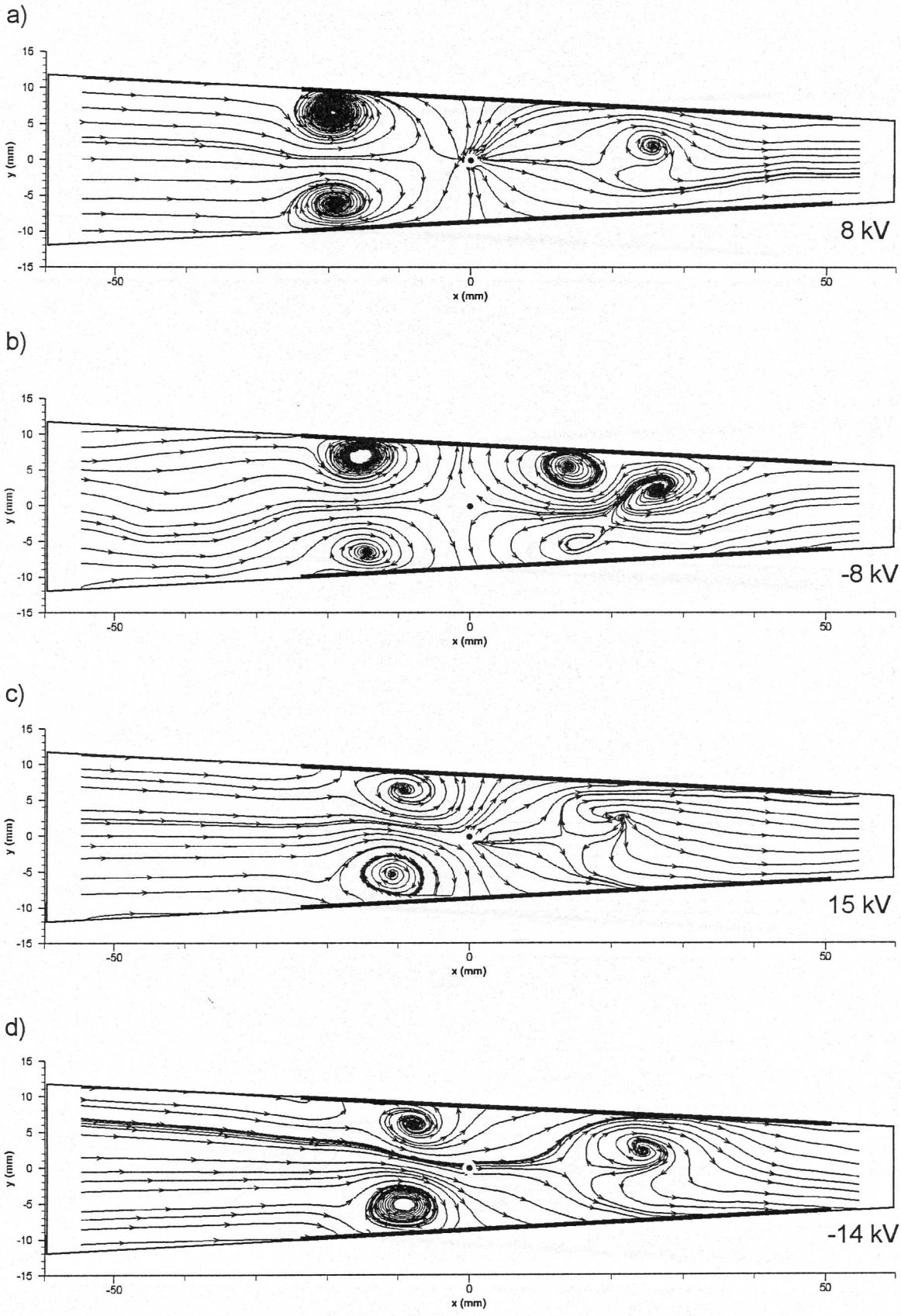

Figure 7. Flow streamlines for PF-B type EHD gas pump; a, c - positive voltage polarity, b, d - negative voltage polarity.

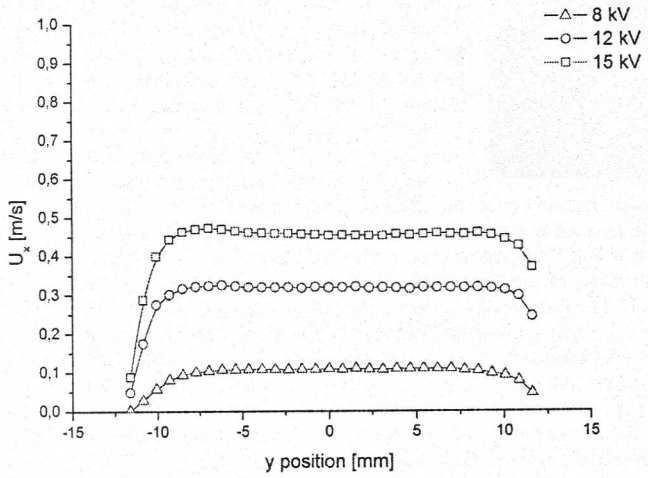

Figure 8. Velocity profiles measured at the inlet section of PF-A type EHD gas pump for positive voltage polarity.

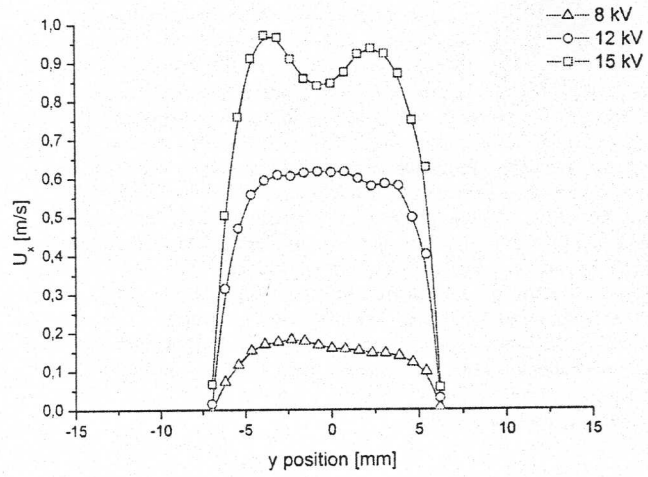

Figure 9. Velocity profiles measured at the exit section of PF-A type EHD gas pump for positive voltage polarity.

Figures 8 and 9 show the crosswise flow velocity profiles for PF-A type EHD gas pump at the pump inlet (x=-54 mm) and the pump exit (x=54 mm), respectively, for the positive voltage polarity. The flow velocity profiles at the pump inlet are relatively flat because the gas entering the EHD pump is not affected yet by the discharge. On the other hand, the gas flow at the pump exit area is strongly disturbed by the vortices formed inside the EHD gas pump and forming non-monotonic M-shaped velocity profile as shown in Fig. 9. Assuming that the profiles of U_x velocity component along the z axis at the pump inlet are similar to the profiles of U_x velocity component along the y axis as shown in Figure 8, then the calculated volumetric flow rates are summarized in Table 1.

4 CONCLUDING REMARKS

The PIV measurement of the gas flow for two different electrode positions in EHD gas pump was performed. The results show that the generated flow patterns are turbulent and with distinct vortices. The vortices decrease with increasing operating voltage. One can deduce from the obtained flow patterns that the flow generated inside the EHD pump is three dimensional. The vortices formed inside the EHD gas pump have negative effect on pumping capabilities of the pump since the vortices may block and suppress the generated flow. The strongest pumping effect (24 L/min) was observed for PF-A type EHD pump at 14-15 kV, when the downstream (Figures 5c-5d) or upstream (Figures 6c-6d) vortices were scattered by the unidirectional flow. However, further optimization of the electrode geometry and discharge parameters is required to minimize the formation of vortices inside the EHD gas pump to improve its pumping capabilities.

ACKNOWLEDGMENT

The authors thank H. Tsubone, G.D. Harvel, C.Y. Ching and K. Urashima for valuable discussion and comments. This work was supported partly by NSERC of Canada and MMO-OCE Inc. (MK, JSC).

REFERENCES

[1] M. Robinson, "Movement of Air in the Electric Wind of the Corona Discharge", Trans. Amer. Inst. Electr. Eng. Vol. 80, pp. 143–150, 1961.

[2] S.H. Jeong and S.S. Kim, "A Study on the Electrohydrodynamic Flow in a Rectangular Impactor with Positive Corona Discharge", Aerosol Sci. Tech., Vol. 29, pp. 1-16, 1998.

[3] L. Leger, E. Moreau, F. Artana and G. Touchard, "Influence of a DC Corona Discharge on the Airflow along an Inclined Flat Plate", J. Electrostat., Vol. 51-52, pp. 300–306, 2001.

[4] R. Ohyama, A. Watson and J.S. Chang, "Electrical Current Conduction and Electrohydrodynamically induced Fluid Flow in an AW Type EHD Pump", J. Electrostat., Vol. 53, pp. 147–158, 2001.

[5] K. T. Hyun and C. H. Chun, "The Wake Flow Control behind a Circular Cylinder Using Ion Wind", Exp. Fluids, Vol. 35, pp. 541–552, 2003.

[6] M. Rickard, D. Dunn-Rankin, F. Weinberg and F. Carleton, "Maximizing Ion-Driven Gas Flows", J. Electrostat., Vol. 64, pp. 368–376, 2006.

[7] J. Ueno, H. Tsubone, B. Komeili, S. Minami, G.D. Harvel, K. Urashima, C. Y. Ching and J. S. Chang, "Flow Characteristics of DC Wire-non-parallel Plate Electrohydrodynamic Gas Pump", Proc. Intern. Sympos. Electrohydrodynamics (ISEHD), Buenos Aires, Argentina, pp. 259-262, 2006.

[8] J. Mizeraczyk, M. Kocik, J. Dekowski, M. Dors, J Podlinski, T. Ohkubo, S. Kanazawa and T. Kawasaki, "Measurements of the Velocity Field of the Flue Gas Flow in an Electrostatic Precipitator Model using PIV method", J. Electrostat., Vol. 51–52, pp. 272–277, 2001.

[9] J. Mizeraczyk, J. Dekowski, J. Podliński, M. Kocik, T. Ohkubo, S. Kanazawa, "Laser Flow Visualization and Velocity Fields by Particle Image Velocimetry in Electrostatic Precipitator Model", J. Visualization, Vol. 6, No. 2, pp. 125-133, 2003.

[10] J. Podliński, J. Dekowski, J. Mizeraczyk, D. Brocilo and J.S. Chang, "Electrohydrodynamic Gas Flow in a Positive Polarity Wire-Plate Electrostatic Precipitator and the Related Dust Particle Collection Efficiency", J. Electrost., Vol. 64, pp. 259-262, 2006.

[11] J. Podliński, J. Dekowski, J. Mizeraczyk, D. Brocilo, K. Urashima and J.S. Chang, "EHD Flow in a Wide Electrode Spacing Spike-Plate Electrostatic Precipitator under Positive Polarity", J. Electrost., Vol. 64, pp. 498 505, 2006.

[12] M. Kocik, J. Dekowski, J. Mizeraczyk, "Particle Precipitation Efficiency in an Electrostatic Precipitator", J. Electrost., Vol. 63, pp. 761-766, 2005.

[13] Y.N. Chun, J.S. Chang, A.A. Berezin and J. Mizeraczyk, "Numerical Modeling of Near Corona Wire Electrohydro-dynamic Flow in a Wire-plate Electrostatic Precipitator", IEEE Trans. Dielectr. Electr. Insul., Vol.14, pp. 119-124, 2007.

[14] J.S. Chang, D. Brocilo, K. Urashima, J. Mizeraczyk, J. Dekowski, J. Podlinski, M. Dors, M. Kocik and T. Ohkubo, S. Kanazawa, Y. Nomoto, "Optimization of seed-particle size and density used in Particle Image Velocimetry under corona discharges and non-thermal plasmas", 7th Int. Congress on Optical Particle Characterization, Kyoto, Japan, pp. 32-37, 2004.

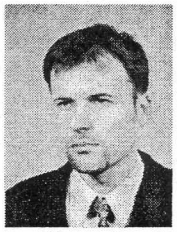

Marek Kocik was born in 1970 in Warsaw, Poland. He graduated in 1996 with M.Sc. degree from the University of Gdańsk in experimental physics in the field of atomic spectroscopy. He received the Ph.D. degree from the Institute of Fluid Flow Machinery, Polish Academy of Sciences in 2002, where he is presently an Assistant Professor. In 2003-04 he was a Fellow of the Japan Society for the Promotion of Science at the Oita University, Japan. In 2006 he was a Visiting Professor in McMaster University, Hamilton, Canada. His research concerns laser applications to micromachining, laser flow diagnostics and laser spectroscopy. He has co-authored 21 refereed papers and presented more than 120 conference papers on these topics.

Janusz Podliński received the M.Sc. degree in electronics and telecommunications at the Technical University of Gdańsk in 2001. He works as an Assistant Researcher at the Institute of Fluid Flow Machinery, Polish Academy of Sciences, Gdańsk, Poland. His research interest concerns fluid and particle flows in electrostatic precipitators and non–thermal plasma reactors, electrohydrodynamics, PIV measurement technique

Jerzy Mizeraczyk received the M.Sc. degree in electronics from the Technical University of Gdańsk in 1966, the Ph.D. degree from the Technical University of Gdańsk in 1976, and Dr. hab. in electrical engineering from the University of Gdańsk in 1988. He was a fellow of the Japan Society for the Promotion of Science at the Nagoya University, Japan, of the A. v.–Humboldt Foundation and H. Hertz Foundation at the Ruhr University Bochum, Germany. He was a Visiting Senior Researcher at the Chalmers University of Technology, Göteborg, Sweden, and at the McMaster University, Hamilton, ON, Canada. He also was a Full Professor at Oita University, Japan. He is currently Professor and Head of the Centre of Plasma and Laser Engineering, Institute of Fluid–Flow Machinery, Polish Academy of Sciences, Gdańsk, Poland. He was a Co–Director of two European Community Copernicus Projects and NATO "Science for Peace Programme" Project. He has worked in the areas of plasma physics, dc, pulsed, RF and MW discharges, lasers and their applications, and plasma chemistry for environmental technologies. He has authored more than 100 refereed papers and presented more than 100 conference papers on these topics.

Jen-Shih Chang (M'90-SM'96) received the B. Eng. and M. Eng. degrees in electrical engineering from Musashi Institute of Technology, Tokyo, Japan, and the Ph.D. degree in experimental space sciences from York University, Toronto, ON, Canada. During 1973-1974, he was a Researcher at the Centre de Recherches en Physique de l'Environment, CNRS, France. From 1975 to 1979, he was a Project Scientist/Assistant Professor with the Department of Physics and Center for Research in Experimental Space Sciences, York University. From 1979 and 1986, he was an Assistant Professor/Associate Professor with the Department of Engineering Physics, McMaster University, Hamilton, Ontario, Canada. From 1985 to 1996, he was a Visiting Professor at Musashi Institute of Technology., Tokyo Denki University, the University of Tokyo, University of Seville, Joseph Fourier University, University of Poitiers, Oita University, and Tokyo University of Agriculture and Technology. Since 1987, He has been a Professor at McMaster University, and is involved in research on applied electrostatics, lightning, air pollution control, and solid and liquid waste destruction plasma technologies. Prof. Chang is currently Chair of the Electrohydrodynamics Technical Committee of the IEEE Dielectrics and Electric Insulation Society.